

## Original Article

# Comprehensive chemical analysis of the flower buds of five *Lonicera* species by ATR-FTIR, HPLC-DAD, and chemometric methods

Yanqun Li<sup>a,b,c,1</sup>, Dexin Kong<sup>a,1</sup>, Hong Wu<sup>a,b,c,\*</sup>



<sup>a</sup> State Key Laboratory for Conservation and Utilization of Subtropical Agro-Bioresources, South China Agricultural University, Guangzhou, China

<sup>b</sup> Guangdong Technology Research Center for Traditional Chinese Veterinary Medicine and Natural Medicine, South China Agricultural University, Guangzhou, China

<sup>c</sup> Guangdong Key Laboratory for Innovative Development and Utilization of Forest Plant Germplasm, South China Agricultural University, Guangzhou 5, China

## ARTICLE INFO

### Article history:

Received 5 March 2018

Accepted 28 June 2018

Available online 21 July 2018

### Keywords:

*Lonicera* species

ATR-FTIR

HPLC-DAD

Chemometrics

Quality evaluation

## ABSTRACT

*Lonicera japonica* Thunb., Caprifoliaceae, has been employed in traditional Chinese medicine for thousands of years. However, it is frequently confused with closely related species, and thus, a mixture of these species is commonly used. The sources of *Lonicera* species must be accurately and rapidly determined to ensure the clinical efficacy of herbal medicines. Attenuated total reflectance Fourier transform infrared spectroscopy and high-performance liquid chromatography with a diode array detector, combined with chemometrics methods, were used to comprehensively evaluate the *Lonicera* quality. The infrared fingerprint results indicated that the spectra of *L. japonica* and its related species were very similar in the range 4000–1800 cm<sup>-1</sup>, however a large number of chemical absorption peaks were observed in the region 1800–600 cm<sup>-1</sup> with certain differences. The five *Lonicera* species had high chlorogenic acid (25.85–67.75 µg/mg), 3,5-di-O-caffeylquinic acid (11.63–62.58 µg/mg), and 4,5-di-O-caffeylquinic acid (2.64–30.91 µg/mg) contents. The chemical fingerprints of *L. hypoglauca* Miq. and *L. confusa* DC were the most similar to that of *L. japonica* Thunb. The chemical fingerprints of *L. fulvotomentosa* P.S. Hsu & S.C. Cheng and *L. macranthoides* Hands.-Mazz. were very different from that of *L. japonica*. A loading analysis indicated that the differences in the chemical fingerprints of the *Lonicera* species were mainly due to variations in the contents of the organic acids and flavonoids. Soft independent modeling of class analogy model was successfully developed to classify unknown samples of the five *Lonicera* species. This comprehensive, unbiased strategy provides adequate, reliable scientific evidence for authenticating herbal sources, therefore offering a powerful, new route for herbal analysis.

© 2018 Sociedade Brasileira de Farmacognosia. Published by Elsevier Editora Ltda. This is an open access article under the CC BY-NC-ND license (<http://creativecommons.org/licenses/by-nc-nd/4.0/>).

## Introduction

*Lonicerae Japonicae Flos* (LJF), the flower buds of *Lonicera japonica* Thunb., Caprifoliaceae, have been used in traditional Chinese medicine to treat exopathogenic wind heat, epidemic febrile diseases, furuncles, sores, carbuncles, and some infectious diseases; they have also been used as cosmetic and food additives, such as those in healthy beverages (Shang et al., 2011, China Pharmacopoeia Commission, 2015a). Recently, the commercial value of LJF in herbal medicine trade markets has increased by more than 400%, and more than 30% of current traditional Chinese medicine prescriptions contain LJF (Yuan et al., 2012). However, because the *Lonicera* L. family comprises 200 species worldwide,

many species are distributed in China. Furthermore, the Chinese Pharmacopeia defined LJF as the flower buds of *L. japonica* and *Lonicerae Flos* (LF) as the flower buds of *L. macranthoides* Hands.-Mazz., *L. hypoglauca* Miq., *L. confusa* DC. (*L. dasystyla* Rheder), and *L. fulvotomentosa* P.S. Hsu & S.C. Cheng (China Pharmacopoeia Commission, 2015a,b), and twelve *Lonicera* species have been used as traditional Chinese medicines for many years in China.

Recently, increasing global demand has resulted in the cultivation of large areas of *L. japonica* and closely related cultivars and landraces (Hu et al., 2011), and many wild *Lonicera* species are also harvested for medicinal and food applications. *L. japonica* and closely related species have been used to produce medicines with similar morphologies but different qualities, which is detrimental to the development of *Lonicera*-based markets. Therefore, a simple, advanced assessment method for differentiating between the complex LJF and LF species must be developed.

Previous studies on the identification of *Lonicera* have mainly focused on the morphology and anatomical characters (Pu et al.,

\* Corresponding author.

E-mail: [wh@scau.edu.cn](mailto:wh@scau.edu.cn) (H. Wu).

<sup>1</sup> These authors contributed equally to this work.

2002; Li et al., 2007; Wang et al., 2014), chemical analysis (Hu et al., 2011; Shang et al., 2011; Yuan et al., 2012), and DNA molecular marker techniques (Wang et al., 2007; Peng et al., 2009; Sun et al., 2011). Although these methods have some advantages, they give little information about the chemical components of herbal medicines, which are complex systems with various compositions. Furthermore, the pharmacodynamic effect of a given herbal medicine is often attributable to several different components. Moreover, only partial information is obtained by a single analytical technique; thus, herbal medicine analysis results do not usually indicate its quality (Liu et al., 2010). Currently, spectrometric (NMR and MS) and chromatographic (TLC, HPLC, and GC) methods are widely used to identify herbal medicines. Additionally, chemometrics has become a popular method for analyzing complex systems because it can resolve overlapping and embedded peaks in spectra and chromatograms and provides a significant amount of information (Su et al., 2008). For example, hierarchical cluster analysis (HCA), principal component analysis (PCA), artificial neural networks (ANNs) and the soft independent modeling of class analogy (SIMCA) method have been used to identify the components of raw medicinal materials (Li et al., 2013, 2016; Custers et al., 2014; Bajpai et al., 2017). Recently, liquid chromatography and mass spectrometry were used to identify *Lonicera* species flower buds (Gao et al., 2012; Seo et al., 2012). Single standard to determine multi-components (SSDMC) combined with PCA was used for the evaluation of *Lonicera* flowers (Gao et al., 2016). These techniques effectively differentiate between subtly different chemical components.

High-performance liquid chromatography-mass spectrometry (HPLC-MS) and gas chromatography-mass spectrometry (GC-MS) are often employed to determine the quality of herbal medicines (Chen et al., 2007; Gao et al., 2012; Seo et al., 2012). However, using these methods for online quality control is not feasible because of the complicated sample preparation procedures and long analysis times required. Moreover, these destructive methods are poorly suited for quality monitoring because they inevitably damage and consume the sample materials. Over the last decade, Fourier transform infrared (FTIR) spectroscopy has become an important technique for quantitative and qualitative analyses because it can detect very low concentrations of the analytes of interest in complex samples, it requires little or no sample preparation, and some of the spectroscopic techniques are non-destructive. This technology can be applied to a wide range of materials and requires small sample volumes and minimal analysis time, which speeds up sample analysis considerably (Edelmann et al., 2001). The feasibility of infrared spectroscopy has recently been demonstrated in the pharmaceutical (Wu et al., 2008), food (Bureau et al., 2009), and agricultural (Aouidi et al., 2012) industries. In the present study, the fingerprints of *L. japonica* and several closely related species were obtained by combining attenuated total reflectance Fourier transform infrared spectroscopy (ATR-FTIR) and HPLC-DAD with chemometric analysis methods, providing comprehensive information about their chemical compositions. This information will be useful for identifying and assessing the quality of *Lonicera* herbal medicines. Understanding the systematic differences between *L. japonica* and closely related species would provide valuable information for ensuring the quality and therapeutic effects of their medicinal products.

## Material and methods

### Plant materials and sample collection

Fresh bud samples of *Lonicera japonica* Thunb., Caprifoliaceae, and closely related species recorded in the Chinese Pharmacopeia

were collected from the main *Lonicera*-producing areas in China. Previous research showed that green alabastra of *Lonicera* species have higher chlorogenic acid and luteoside contents (Kong et al., 2017); thus, all the collected samples were green alabastra. The samples were authenticated by Prof. Qin-er Yang (South China Botanical Garden, Chinese Academy of Sciences). Voucher specimens were deposited in the herbarium of the Department of Botany at South China Agricultural University. Table 1 lists details about the sample collection.

Each of the five *Lonicera* species studied in this work were collected from four different major production areas. Eight samples were collected at each location. The samples were dried according to the methods of Kong et al. (2017) and then stored in a drying oven until analysis.

### HPLC-DAD analysis

HPLC analysis was performed according to the methods of Kong et al. (2017). An accurately weighed powder sample (0.1 g) was suspended in 25 ml of 50% methanol (v/v), ultrasonically extracted for 40 min, and then cooled to room temperature; 50% methanol was added to compensate for lost weight. The mobile phase comprised solvents A (acetonitrile) and B (0.05%  $\text{H}_3\text{PO}_4$ ) in the following separation program: 0–21 min (10–17% A), 21–33 min (17–23% A), and 33–43 min (23–26% A). The number of theoretical plates was  $\geq 3000$ , and the flow rate was maintained at  $0.5 \text{ ml min}^{-1}$ . The detection wavelength was set to 327 nm. Each sample injection (5  $\mu\text{l}$ ) was performed in triplicate for statistical analysis. The chromatographic peaks were identified by comparing the retention times. Quantification of the single compound was directly performed by HPLC/DAD using a five-point regression curve built with the available standards.

5-Caffeoylquinic acid (5-CQA) (906-33-2), chlorogenic acid (CGA) (327-97-9), 4-caffeoylequinic acid (4-CQA) (905-99-7), caffeoic acid (331-39-5), rutin (153-18-4), hyperoside (482-36-0), luteoloside (5373/11/5), 3,4-di-O-caffeoylequinic acid (3,4-di-O-CQA) (14534-61-3), 3,5-di-O-caffeoylequinic acid (3,5-di-O-CQA) (2450-53-5), and 4,5-di-O-caffeoylequinic acid (4,5-di-O-CQA) (32451-88-0) reference standards were purchased from Chengdu Must Bio-Technology Co., Ltd. (China). The calibration plots of the 10 standards were constructed from the peak areas ( $y$ ) obtained for six different concentration solutions ( $x$ ). The best-fit standard curves were obtained by linear regression of the peak area versus concentration plots, and all of them exhibited good linearity ( $R^2 > 0.999$ ) over a relatively wide concentration range.

### ATR-FTIR analysis

A Nicolet 6700 FTIR spectrometer (Thermo Nicolet Corp.) equipped with a Smart iTR accessory for ATR sampling (Thermo Fisher Scientific, Madison, WI, USA) and a deuterated triglycine sulfate (DTGS) detector was employed in the ATR-FTIR experiments. The Smart iTR accessory was equipped with a single-bounce diamond crystal. The Spectrum IR software package was used to collect data in the wavenumber range from 4000 to 600  $\text{cm}^{-1}$  at a spectral resolution of  $4 \text{ cm}^{-1}$ . The room was maintained at ambient temperature ( $25^\circ\text{C}$ ) and relative humidity (30%). The dry sample powder (2 mg) was coated onto the crystal to a thickness of approximately 0.2 mm for the infrared spectroscopic analysis. After each measurement, the crystal was cleaned using a soft tissue soaked with methanol and left to dry in ambient air. The each sample measurement was replicated five times, and then the average chart was taken as a last sample spectrum. The background air, water vapor, and  $\text{CO}_2$  interference spectra were subtracted from these spectra.

**Table 1**  
*Lonicera* germplasm samples and collection sites.

Species	Voucher No.	Sample	No.	Location	Collection date	Gatherer
<i>L. japonica</i>	SCJ20140601	A	S <sub>1</sub>	Fengqiu, Henan, China	June 2014	Yanqun Li, Dexin Kong
	SCJ20140602		S <sub>2</sub>	Xinyang, Henan, China	June 2014	Yanqun Li, Dexin Kong
	SCJ20140603		S <sub>3</sub>	Guilin, Guangxi, China	June 2014	Yanqun Li, Dexin Kong
	SCJ20140604		S <sub>4</sub>	Guangzhou, Guangdong, China	June 2014	Yanqun Li, Dexin Kong
<i>L. confusa</i>	SCC20140601	B	S <sub>5</sub>	Guangzhou, Guangdong, China	June 2014	Yanqun Li, Dexin Kong
	SCC20140602		S <sub>6</sub>	Zengcheng, Guangdong, China	June 2014	Dexin Kong
	SCC20140603		S <sub>7</sub>	Nanning, Guangxi, China	June 2014	Yanqun Li, Dexin Kong
	SCC20140604		S <sub>8</sub>	Hengxian, Guangxi, China	June 2014	Dexin Kong
<i>L. fulvotomentosa</i>	SCF20140701	C	S <sub>9</sub>	Baise, Guangxi, China	July 2014	Yanqun Li, Xiaodong Yan
	SCF20140702		S <sub>10</sub>	Longling, Guangxi, China	July 2014	Dexin Kong, Xiaodong Yan
	SCF20140703		S <sub>11</sub>	Baise, Guangxi, China	July 2014	Dexin Kong, Xiaodong Yan
	SCF20140704		S <sub>12</sub>	Nanning, Guangxi, China	July 2014	Dexin Kong
<i>L. macranthoides</i>	SCM20140701	D	S <sub>13</sub>	Nanning, Guangxi, China	July 2014	Yanqun Li, ManlianWang
	SCM20140702		S <sub>14</sub>	Guilin, Guangxi, China	July 2014	Yanqun Li, ManlianWang
	SCM20140601		S <sub>15</sub>	Ziyuan, Guangxi, China	June 2014	Dexin Kong, ManlianWang
	SCM20140601		S <sub>16</sub>	Longhui, Hunan, China	June 2014	Dexin Kong
<i>L. hypoglauca</i>	SCH20140601	E	S <sub>17</sub>	Mashan, Guangxi, China	June 2014	Yanqun Li, ManlianWang
	SCH20140602		S <sub>18</sub>	Guilin, Guangxi, China	June 2014	Zongyou Chen, Rong Zou
	SCH20140603		S <sub>19</sub>	Lingui, Guangxi, China	June 2014	Zongyou Chen, Rong Zou
	SCH20140604		S <sub>20</sub>	Nanning, Guangxi, China	June 2014	Dexin Kong, Shugen Wei

### Pre-processing of the data

To avoid enhancing the noise, which is a consequence of derivative, spectra are first smoothed. This smoothing is done by using the Savitzky–Golay algorithm, which is a moving window averaging method: a window is selected where seven points are fitted by a polynomial of a certain degree. The central point in the window is replaced by the value of the polynomial. Secondly, a baseline correction algorithm was applied for automatically removing baseline contributions from the data. It subtracts a baseline from a chromatogram using an iterative asymmetric least-squares procedure. Points with residuals <0 are up-weighted at each iteration of the least-squares fitting. This results in a robust “non-negative” residual fit when residuals of significant amplitude are present (Massart et al., 2007). Smoothing and baseline correction were performed using the OMNIC 8.3 software (Thermo Fisher Scientific, Madison, WI, USA).

### Principal component analysis

PCA was performed by singular-value decomposition of the fingerprint data array. One of the goals of PCA is to reduce the number of variables to enable visualization of the information in the multivariate data set (Gemperline, 2006). In PCA, a linear combination of the original variables is constructed to obtain principal components while preserving the largest possible variation in X. Score plots are used to visualize object similarities and clustering tendencies, whereas loading plots reveal the contributions of the original variables (Tistaert et al., 2009).

For each species, 10 average spectra were applied in this analysis. The original variables are replaced by a few principal-component variables (PCs). The PCs are totally independent of each other and ordered so that the first factors contain most of the original variation, the second factors contain the second largest amounts, etc. The PCs were calculated from scaled and centered variables so that every factor has the same impact on each PC. The Unscrambler 9.7 (CAMO, Norway) and Origin 9.0 (MicroCal, USA) software programs were used to perform PCA in this work.

### Hierarchical cluster analysis

HCA is a cluster analysis method that seeks to build a cluster hierarchy. Any valid metric can be used to determine the similarity between pairs of observations. Thus, samples within a cluster

have many similarities, whereas samples in different clusters are dissimilar (Buchgraber et al., 2004). For each species, ten average spectra were also applied for cluster analysis of FTIR fingerprint. HCA and the Euclidean distance were employed in this study. The distance matrix was constructed from the chromatographic areas of the samples for the cluster analysis of the HPLC-DAD data, whereas the relative absorption was selected as the metric for the cluster analysis of the FTIR data. The SPSS version 18.0 software (SPSS Inc., Chicago, USA) was used to perform the cluster analysis and to construct the dendrogram of the results.

### Soft independent modeling by class analogy

Soft independent modeling by class analogy (SIMCA) is a well-known multivariate supervised pattern recognition method based on PCA. SIMCA considers different classes which are modeled individually by a separate principal component model. The spectra were imported into the Assure Unscrambler 9.7 software package to perform a SIMCA analysis. In the present work, five species were defined: (A) *L. japonica*, (B) *L. confusa*, (C) *L. fulvotomentosa*, (D) *L. macranthoides*, and (E) *L. hypoglauca*. The following equations mathematically describe the more detailed procedure of SIMCA (Beebe et al., 1998; Park et al., 2007):

$$S_0^k = \left[ \sum_{j=1}^m \sum_{i=1}^{n_k} \frac{(e_{ij}^k)^2}{(n_k - p_k - 1)(m - p_k)} \right]^{1/2}$$

$$S_u^k = \left[ \sum_{j=1}^{m_k} \frac{(e_{uj}^k)^2}{(m - p_k)} \right]^{1/2}$$

$$F = \frac{(S_u^k)^2}{(S_0^k)^2}$$

$$(S_{\text{lim}}^k) = (S_0^k) F^{0.05}$$

Here  $S_0^k$  is the standard deviation of the training set for the class  $k$ ,  $n_k$  is the number of objects,  $p_k$  is the number of significant principal components in class  $k$ ,  $m$  is the number of variables, and  $e_{uj}^k$  is the residual. The standard deviation of the unknown spectrum,  $S_u^k$ , is

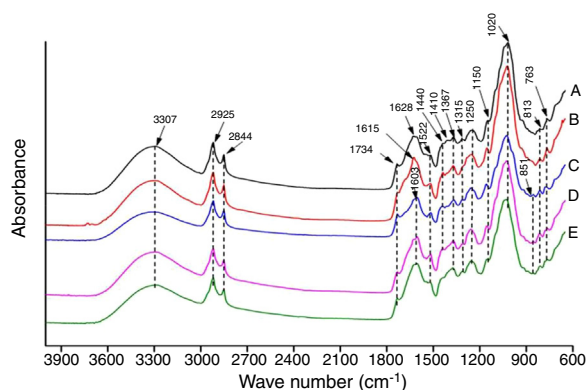


**Figure 1.** ATR-FTIR spectra of the five *Lonicera* species. (A) *L. japonica*; (B) *L. confusa*; (C) *L. fulvotomentosa*; (D) *L. macranthoides*, and (E) *L. hypoglauca*.

then calculated using the  $e_{ij}$  value. In SIMCA, an unknown spectrum is identified as a specific group by comparing the  $F$ -distribution with the 99% confidence interval. If the  $F$  value is larger than the critical  $F$  value at a given level of significance, one can conclude that the interclass distance ( $u$ ) from class  $K$  is significantly larger than that of class  $K$  as a whole and is to be excluded from class  $K$ . If the distance is not significantly larger than the  $F$  value, the sample is determined to be a member of class  $K$ . Predetermined classes ( $K=L. japonica$ , *L. confusa*, *L. fulvotomentosa*, *L. macranthoides*, and *L. hypoglauca*) calculated with 99% confidence intervals were projected onto three-dimensional PCA scores plots, using the first three principal component scores as axes, so the separation of classes could be easily perceived with the spectral variance captured.

The ATR-FTIR spectra of 32 samples of each species were used to build the SIMCA model. The SIMCA model training set consisted of 90 ATR-FTIR spectra of *L. japonica*, *L. confusa*, *L. fulvotomentosa*, *L. macranthoides*, and *L. hypoglauca* (18 spectra of each class), and the other 70 unknown samples were used to evaluate the training set. When a SIMCA model is employed to analyze unknown samples (prediction), the samples are compared to the defined classes and assigned to a class based on their similarity to the defined classes. A unique feature of SIMCA is that the unknown sample can be assigned to one or more classes or none of the classes. Classification is based on the interclass distances between the unknown and defined classes. In this study, the performances of the developed SIMCA models were evaluated on the basis of the interclass distances between the different defined classes and the recognition and rejection of the samples used to validate the models.

## Results and discussion

### ATR-FTIR fingerprint analysis

The characteristic IR fingerprints of the *Lonicera* samples were obtained in the range 4000–600 cm<sup>-1</sup> (Fig. 1); typical spectra are shown in Fig. 1. The spectra were analyzed, and several characteristic peaks were observed. The peak at 3307 cm<sup>-1</sup> was assigned to the –OH deformation mode, and the peaks at 2925 and 2844 cm<sup>-1</sup> were attributed to the CH<sub>3</sub>- and CH<sub>2</sub>- stretching vibrations, respectively. The peaks at 1734, 1627, 1522, 1440, 1410, 1367, 1315, and 1255 cm<sup>-1</sup> corresponded to chlorogenic acid and flavonoids, and the peaks at 1734, 1627, and 1522 cm<sup>-1</sup> corresponded to polyphenol carbonyl (C=O) stretching and aromatic ring skeletal (C=C) vibrations. The peaks at 1440, 1410, and 1376 cm<sup>-1</sup> were attributed to organic acid OH vibrational modes. The peaks at 1315 and 1250 cm<sup>-1</sup> were attributed to C–O stretching vibrations, and the peaks at 1150 and 1020 cm<sup>-1</sup> were assigned to –OH deformation

modes. However, as shown in Fig. 1, the spectra of *L. japonica* and its related species were very similar in the range 4000–1800 cm<sup>-1</sup>, and the characteristic IR fingerprint peaks that indicate the chemical composition were mostly in the range 1800–600 cm<sup>-1</sup>. Moreover, the chemical compositions of the five species were very complex and diverse. Because the chemical composition fingerprints strongly overlapped, identifying the differences between the components of these samples was difficult. Thus, several chemometric methods, including PCA and HCA, were used to improve the characterization potential of the fingerprint region (1800–600 cm<sup>-1</sup>) by statistically analyzing the chemical compositions to effectively identify the components.

### PCA and HCA of the ATR-FTIR fingerprints

PCA is a projection method that extracts spectral information and uses the maximum variance principle to fit linear functions of multiple independent variables to the original spectral data. This method reduces the data dimensions because the new low-dimensional variables are used instead of the original high-dimensional variables (Abdi and Williams, 2010; Kim et al., 2012). Fig. 2a shows a two-dimensional scatter plot of the principal components PC1 and PC2 obtained from the IR spectra of the different *Lonicera* samples after PCA. The PC1 components have the highest data variance, with a variance contribution ratio of 89%, followed by the PC2 components with variance contribution rates of 7%. Therefore, the first two principal components reflect the vast majority of the spectral information (which explains 96% of the total variance). All the samples were located in relatively independent positions in principal component space and could thus be effectively distinguished from each other, as shown in Fig. 2a for samples A (*L. japonica*), B (*L. confusa*), C (*L. fulvotomentosa*), D (*L. macranthoides*), and E (*L. hypoglauca*). Samples A (*L. japonica*) and B (*L. confusa*) were separated by a small distance, as were samples D (*L. macranthoides*) and E (*L. hypoglauca*). The distances between sample C (*L. fulvotomentosa*) and the other four samples in the scatter plot were the largest, indicating that the IR spectral characteristics of sample C (*L. fulvotomentosa*) were considerably different from those of the other four samples.

To more directly observe the relationship between and heredity of the different *Lonicera* species, the components of the five species were analyzed using HCA. As shown in Fig. 2b, these results were consistent with the PCA results. When the critical value was  $11 < d < 17$ , the five *Lonicera* species were divided into three main clusters. Because of their small distance coefficients, samples A (*L. japonica*) and B (*L. confusa*) were classified as one cluster, as were samples D (*L. macranthoides*) and E (*L. hypoglauca*). The last cluster consisted of sample C (*L. fulvotomentosa*). Both PCA and HCA showed that samples A (*L. japonica*) and B (*L. confusa*) and samples D (*L. macranthoides*) and E (*L. hypoglauca*) had similar chemical compositions and that they were obviously dissimilar from sample C (*L. fulvotomentosa*). This characteristic distribution of the phytochemicals in *Lonicera* species was similar to that obtained by Wang et al. (2014), who reported that the genetic relationships between *L. macranthoides* and *L. hypoglauca* are very close. Gao et al. (2012) also reported that the chemical components of *L. fulvotomentosa* and *L. macranthoides* exhibited significant differences and that those of *L. japonica* and *L. confusa* were similar. Furthermore, they found that the leaf morphology of *L. japonica* varies from those of closely related plant species but is similar to that of *L. confusa* and that *L. japonica* and *L. confusa* leaves are smaller than those of *L. fulvotomentosa* and *L. macranthoides*. Therefore, the IR spectral variations between *L. japonica* and closely related plant species were assumed to strongly depend on genetic factors.

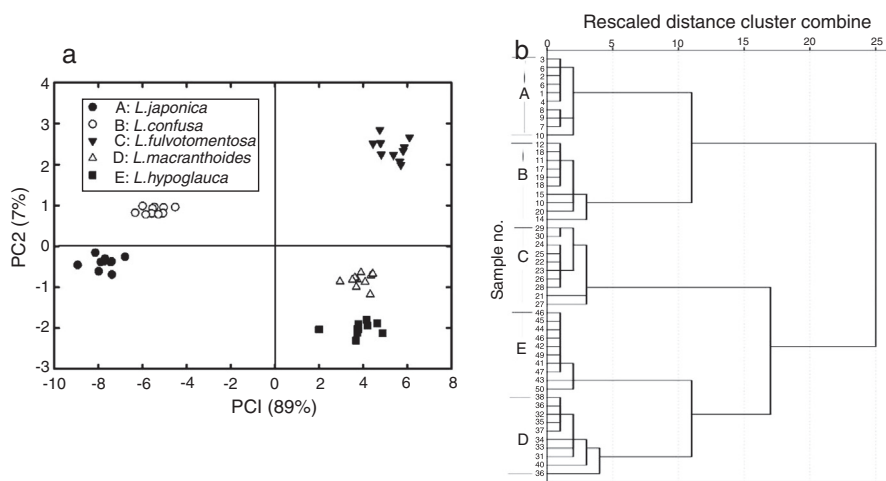


**Figure 2.** (A) Scatter score plot of PC1 and PC2 for the flower buds of *Lonicera japonica* and closely related species; (B) HCA of the ATR-FTIR fingerprints of the flower buds of *L. japonica* and closely related species. (A: *L. japonica*, B: *L. confusa*, C: *L. fulvotomentosa*, D: *L. macranthoides*, and E: *L. hypoglauca*).

#### Loading analysis of *Lonicera* species FTIR fingerprints

The loadings are measures of the weights of the original variables, meaning that the loading of a variable increases with its contribution to the construction of a given principal component (Deconinck et al., 2012). Recently, loading factors have been used in PCA models to effectively detect counterfeit medicines and products and to assess food quality (Li et al., 2013; Demir et al., 2015; Gok et al., 2015). To obtain more information about the differences between the chemical components of various *Lonicera* species using the PCA model, the loading factors were extracted and used to construct a loading factor atlas in the range 1800–700 cm<sup>-1</sup>, as shown in Fig. 3a. Some of the less sensitive absorption peaks were not shown in Fig. 1, whereas these peaks are shown in Fig. 3a. For instance, 1682, 1639, 1471, 1284, 1181, 1111, 1032, 982, 950, 822, and 789 cm<sup>-1</sup>, these peaks were attributed to organic acids and flavonoids (Sun et al., 2010; Zhu et al., 2014; Wang et al., 2015). The first principal components (PC1) are the most important ingredient, and its variance contribution ratio is 89.0%. This indicates that the PC1 can reflect the vast majority of spectrum information. The peaks at 1682 and 1636 cm<sup>-1</sup> (Fig. 3b) corresponded to chlorogenic acid carbonyl (C=O) stretching and aromatic ring skeletal (C=C) vibrations. Compared to the patterns of two-dimensional scatter plot and the loading factor model, samples C–E in Fig. 2a are positively correlated with the peaks of 1748, 1682, 1639, 1471, 1445, 1152, and 950 cm<sup>-1</sup> in Fig. 3a, but it is negatively correlated with sample A. This indicated that samples C–E are rich in phenolic acids, such as chlorogenic acid. As shown in Fig. 3c, the luteoloside vibrational modes are mostly at the peaks of 1602 and 1029 cm<sup>-1</sup>, and sample A in Fig. 2a had the greatest positive correlation with the peaks of 1600 and 1032 cm<sup>-1</sup> in Fig. 3a, but it is negatively correlated with samples C–E. This indicated that the luteoloside content of samples A is higher than that of samples C–E. These results indicate that the differences in the chemical compositions of *L. japonica* and its closely related species are mainly due to variations in the organic acid and flavone contents.

#### Cluster analysis of the HPLC fingerprints

Organic acids and flavonoids are the main components of *Lonicera* species (China Pharmacopoeia Commission, 2015a,b). To verify the accuracy of the ATR-FTIR results for organic acids and flavonoids among the different samples, HPLC-DAD was used to determinate and analyze the fingerprint pattern and content differences of organic acids and flavonoids in *L. japonica* and closely

related species. The data were imported into the Similarity Evaluation System for Chromatographic Fingerprint of Traditional Chinese Medicine software (China Pharmacopoeia Committee, version 2004A). The absorption patterns of all the samples were very similar (Fig. 4a). Ten absorption peaks of seven phenolic acid and three flavonoid standards were observed in this analysis (Fig. 4b). Seven organic acids were identified in all samples, while there still have some differences in flavonoids. For example, samples A (*L. japonica*) and C (*L. fulvotomentosa*) were three flavones, while samples D (*L. macranthoides*) and E (*L. hypoglauca*) were only identified one flavone (Table 2). To more directly observe the relationship between and heredity of the different *Lonicera* species, the HPLC-DAD data were analyzed by HCA. The results obtained from the cluster analysis of the HPLC-DAD data were mostly consistent with those obtained from the cluster analysis of the FTIR fingerprint region. As shown in Fig. 5, when the critical value was 3 < d < 21, the samples were divided into three main clusters: samples A (*L. japonica*), B (*L. confusa*), and E (*L. hypoglauca*); sample C (*L. fulvotomentosa*); and sample D (*L. macranthoides*), indicating that the organic acids and flavonoids of *L. japonica*, *L. confusa*, and *L. hypoglauca* were similar, whereas those of *L. fulvotomentosa* and *L. macranthoides* were obviously dissimilar. These results differ from the FTIR clustering analysis results; the IR spectral data of samples A (*L. japonica*) and E (*L. hypoglauca*) were dissimilar, demonstrating that the two samples had similar organic acids and flavonoids. These results further demonstrated that ATR-FTIR data could feasibly be combined with PCA and loading analysis to obtain accurate results for effectively identifying and monitoring the quality of *L. japonica* and its closely related species.

#### Organic acid and flavonoid content analysis

The active components of *Lonicera* species are secondary metabolites produced during secondary metabolism and differ among species (Xu et al., 1988; Hu et al., 2011). To further compare the content differences in the polyphenol chemical compositions of *L. japonica* and closely related species, the chemical compositions of the five *Lonicera* species were determined and analyzed by HPLC-DAD. The results are expressed as the mean values of the four locations from which the samples were obtained (Table 2). The five *Lonicera* species had similar chemical compositions and mainly consisted of organic acids and flavonoids. CGA and luteoloside are considered the major bioactive constituents of *Lonicera* species (China Pharmacopoeia Commission, 2015a,b). Significant differences were observed in the chemical component contents of

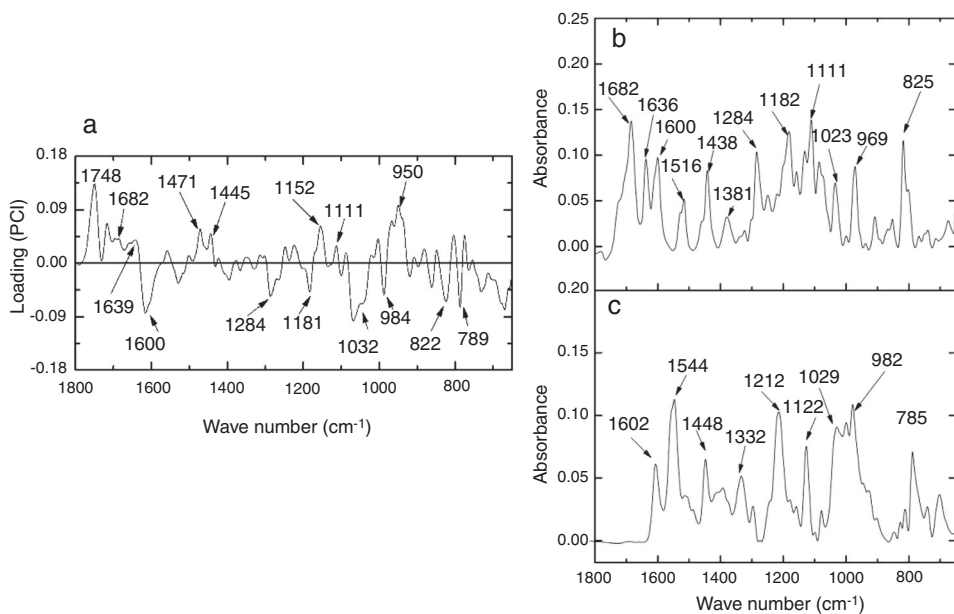


**Figure 3.** (A) PCA loading factors obtained for the flower buds of *Lonicera japonica* and closely related species CGA; (B) Luteoloside; (C) ATR-FTIR fingerprints.

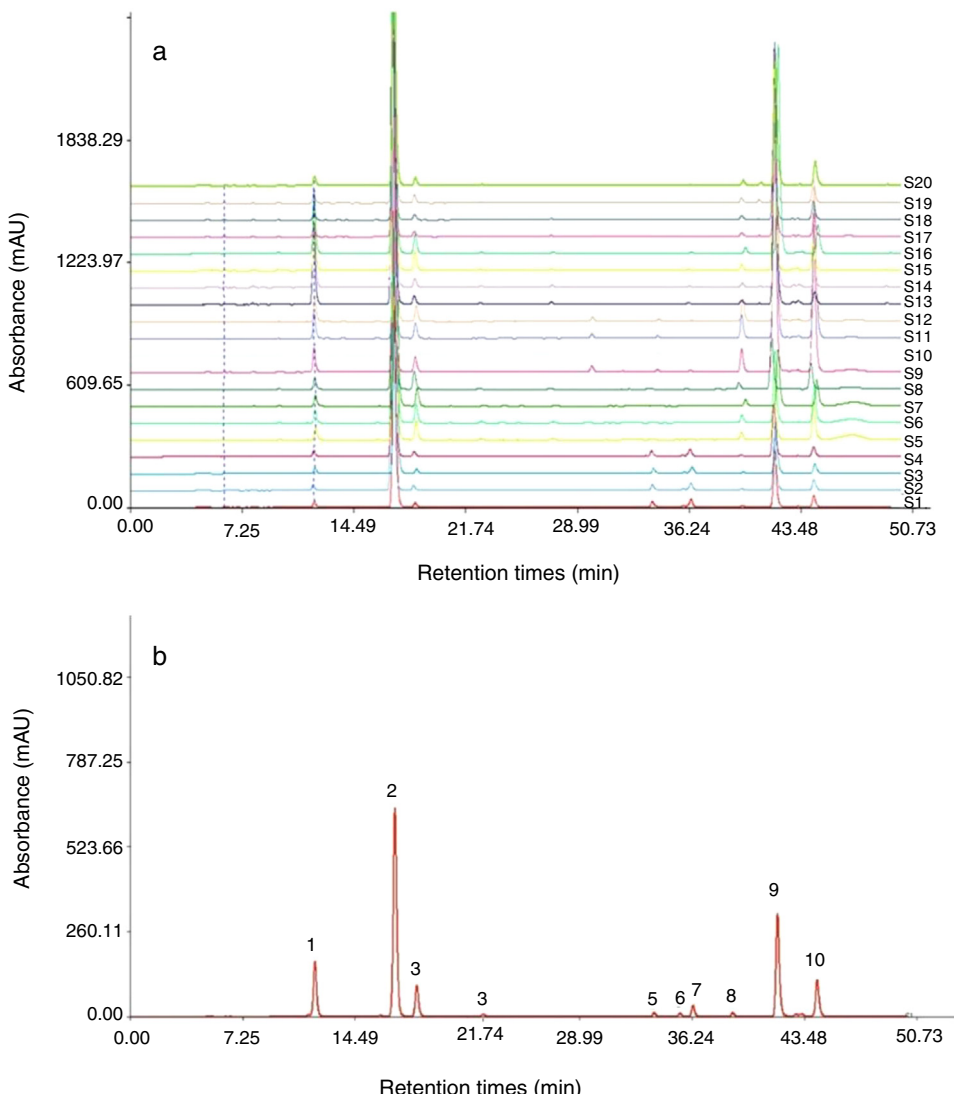


**Figure 4.** (a) HPLC fingerprints of the buds of *Lonicera japonica* and closely related species. (b) Mixture of seven phenolic acid and three flavonoid standards. Peaks 1, 2, 3, 4, 5, 6, 7, 8, 9, and 10 correspond to 5-CQA, CGA, 4-CQA, caffeic acid, rutin, hyperoside, luteoloside, 3,4-di-O-CQA, 3,5-di-O-CQA, and 4,5-di-O-CQA, respectively.

**Table 2**Organic acid and flavonoid contents of the five *Lonicera* species ( $\mu\text{g}/\text{mg}$ ).

Component	A	B	C	D	E
5-CQA	0.32 ± 0.004e	0.61 ± 0.021c	1.18 ± 0.006b	3.49 ± 0.035a	0.45 ± 0.037d
CGA	34.88 ± 0.239c	47.75 ± 2.861b	25.85 ± 0.429e	67.75 ± 3.483a	31.72 ± 2.313d
4-CQA	0.31 ± 0.018c	1.09 ± 0.039a	0.91 ± 0.0115b	0.85 ± 0.034b	0.43 ± 0.012c
Caffeic acid	0.021 ± 0.0004d	0.035 ± 0.0003bc	0.023 ± 0.0004bc	0.042 ± 0.0003a	0.030 ± 0.0009bc
Rutin	0.028 ± 0.001b	0.036 ± 0.003a	0.012 ± 0.0071b	—	—
Hyperoside	0.29 ± 0.005a	—	0.13 ± 0.003b	—	—
Luteoloside	1.56 ± 0.079a	0.077 ± 0.003e	0.26 ± 0.025c	0.21 ± 0.016d	0.71 ± 0.001b
3,4-di-O-CQA	0.170 ± 0.005e	0.765 ± 0.038b	2.584 ± 0.017a	0.573 ± 0.069c	0.494 ± 0.040d
3,5-di-O-CQA	11.63 ± 0.146e	13.77 ± 0.629d	62.58 ± 0.958a	49.28 ± 4.321b	23.86 ± 3.324c
4,5-di-O-CQA	2.64 ± 0.066e	7.07 ± 0.069b	30.91 ± 0.483a	4.51 ± 0.194d	4.88 ± 0.015c

A: *L. japonica*, B: *L. confusa*, C: *L. fulvotomentosa*, D: *L. macranthoides*, and E: *L. hypoglauca*. The values represent the mean ± standard deviation ( $n=3$ ), and the same letters indicate no significant differences among the samples ( $p < 0.05$ ).

the various species. The contents of organic acids, such as CGA, 3,5-di-O-CQA, and 4,5-di-O-CQA, were higher than those of the other components for all the samples. *L. macranthoides* had the highest CGA content (67.75  $\mu\text{g}/\text{mg}$ ), followed by *L. confusa* (47.75  $\mu\text{g}/\text{mg}$ ), whereas *L. fulvotomentosa* had the lowest CGA content of only 25.85  $\mu\text{g}/\text{mg}$ . The 3,5-di-O-CQA and 4,5-di-O-CQA contents of *L. fulvotomentosa* were 62.58 and 30.91  $\mu\text{g}/\text{mg}$ , respectively, and were significantly higher than those of the other four species. *L. japonica* had the lowest 3,5-di-O-CQA and 4,5-di-O-CQA contents (11.63 and 2.64  $\mu\text{g}/\text{mg}$ , respectively). The 5-CQA (0.32–3.48  $\mu\text{g}/\text{mg}$ ), 4-CQA (0.31–1.09  $\mu\text{g}/\text{mg}$ ), 3,4-di-O-CQA (0.17–2.58  $\mu\text{g}/\text{mg}$ ), and caffeic acid (0.02–0.04  $\mu\text{g}/\text{mg}$ ) contents were very low for all five species studied. The flavonoid contents of these *Lonicera* species were also relatively low. Rutin was only detected in *L. japonica* (0.028  $\mu\text{g}/\text{mg}$ ), *L. confusa* (0.036  $\mu\text{g}/\text{mg}$ ), and *L. fulvotomentosa* (0.012  $\mu\text{g}/\text{mg}$ ), and hyperoside was only detected in *L. japonica* and *L. fulvotomentosa* (0.29 and 0.13  $\mu\text{g}/\text{mg}$ , respectively) (Table 2). *L. japonica* and *L. hypoglauca* had high luteoloside contents (1.56 and 0.71  $\mu\text{g}/\text{mg}$ , respectively), whereas the luteoloside contents of *L. confusa*, *L. fulvotomentosa*, and *L. macranthoides* ranged from 0.08 to 0.26  $\mu\text{g}/\text{mg}$  (Table 2). These results are consistent with those of Wang et al. (2014) and Li et al. (2007) that *L. confusa*, *L. fulvotomentosa*, and *L. macranthoides* had low luteoloside contents. The study indicated that the five *Lonicera* species studied are rich in CGA, 3,5-di-O-CQA, and 4,5-di-O-CQA. *L. japonica* and *L. hypoglauca* had relatively high CGA and luteoloside contents. In particular, the CGA and luteoloside contents (3.17 and 0.071%, respectively) of *L. hypoglauca* were much higher than the minimum values (1.5 and 0.050%, respectively) listed for *L. japonica* in the Chinese Pharmacopoeia (China Pharmacopoeia Commission, 2015b). Although the chemical fingerprint of *L. confusa* is similar to that of *L. japonica*, *L. confusa* had a low luteoloside content. Therefore, on the basis of the CGA and luteoloside levels, *L. hypoglauca* could be used as LJF raw material in traditional Chinese medicine.

#### Classification of *Lonicera* species using soft independent modeling of class analogies (SIMCA)

Soft independent modeling of class analogies (SIMCA) is a nonlinear method for multivariate classification based on PCA modeling (Wold, 1976). SIMCA is a superior pattern recognition method in chemometrics. SIMCA considers different classes which are modeled individually by a separate principal component model. A SIMCA model reveals whether an unknown sample belongs to a set of known samples as defined by the calibration set and is therefore useful for authenticating herbal samples. Fig. 6a shows the identification of the subgroup A and B validation set samples (which belong to the subgroup A and B database) and subgroup C–E prediction set samples (which do not belong to the subgroup A and B database). The nearest subgroup A and B class for each “unknown” sample

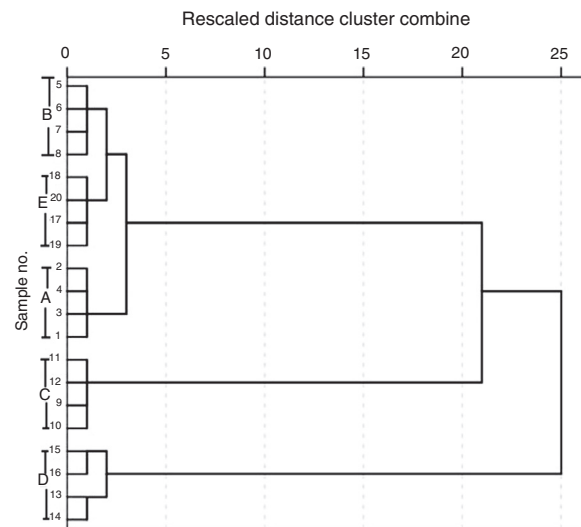


**Figure 5.** HCA of the HPLC-DAD fingerprints of the flower buds of *Lonicera japonica* and closely related species.

was determined by the SIMCA model. None of the subgroup C–E samples were placed in the classes defined by the subgroup A and B calibration set (Fig. 6a). Likewise, Fig. 6b and c shows the identification of the subgroup C and D validation set samples and subgroup E validation set samples, respectively. On the basis of the SIMCA model (Fig. 6a–c), the five prediction subgroup (A–E) samples were distributed in five different areas, i.e., 100% of the 110 calibration set samples and 90 validation set samples were correctly identified by the SIMCA model. The purpose of this experimental design was to test the stability of the SIMCA models, that is, to determine if different herbal medicines could be identified by SIMCA models constructed from different herb combinations. The results showed that the herbs could indeed be rapidly and accurately identified by SIMCA models constructed from different herb combinations.

In this work, HPLC-DAD and ATR-FTIR were combined with statistical classification methods to successfully discriminate between and classify five *Lonicera* species. The analyses revealed that not only is the chemical fingerprint of *L. hypoglauca* similar to that of *L. japonica*, but *L. hypoglauca* also has higher CGA and luteoloside contents and can therefore be considered a promising alternative to LJF in folk medicines. Although the chemical fingerprint of *L. confusa* is similar to that of *L. japonica*, *L. confusa* has a low luteoloside content. Additionally, *L. fulvotomentosa* and *L. macranthoides* differed from *L. japonica*. Therefore, the use of these three species as replacements or supplements in traditional Chinese medicines based on LJF should be cautiously considered. Moreover, all five species were objectively classified by SIMCA models based on IR macro-fingerprints, with excellent recognition rates, and these

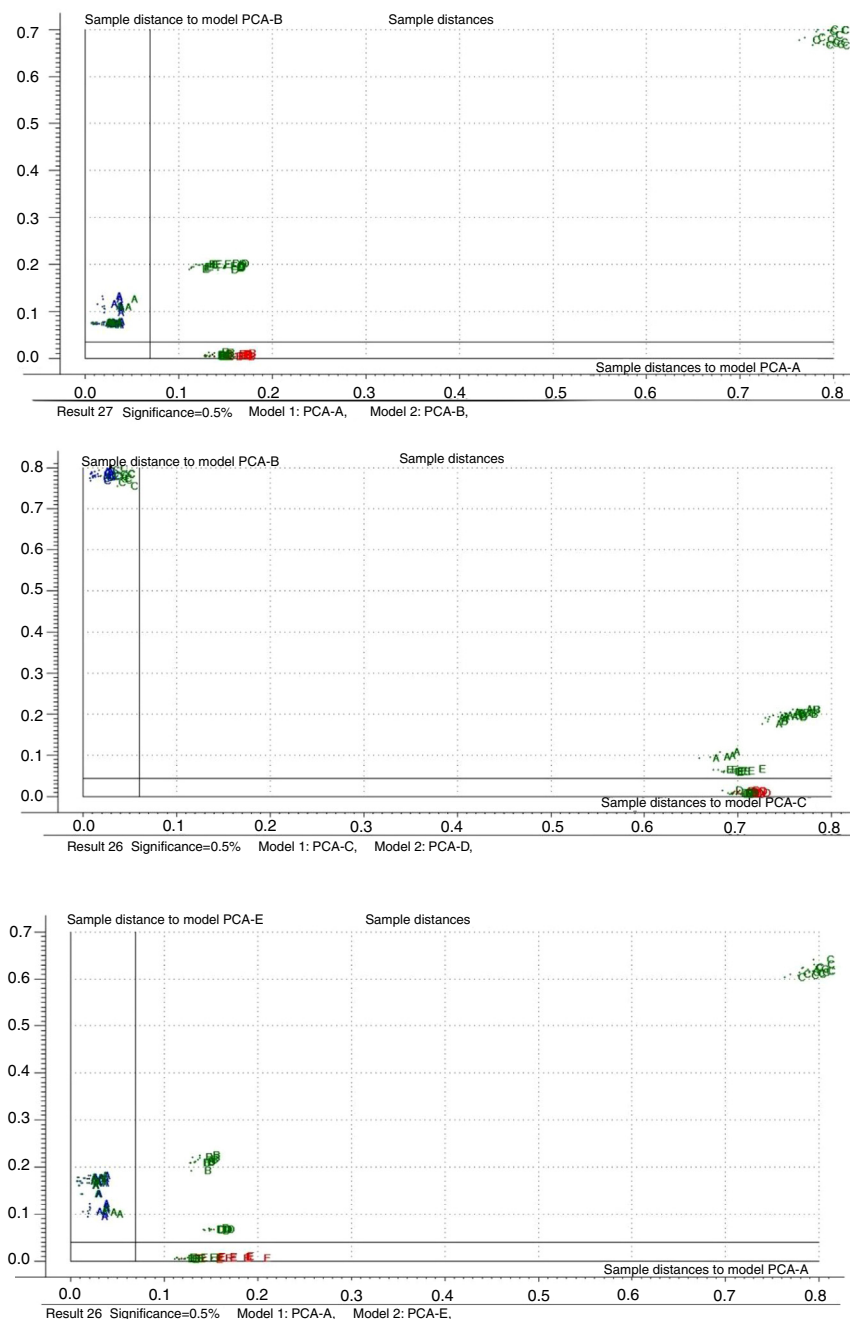


**Figure 6.** Plot of the sample-to-model distances for models A and B (a), C and D (b), and E (c) obtained from the SIMCA classification.

models exhibited good predictive capabilities. Thus, this method offers an effective route for rapidly discriminating between *Lonicera* species and monitoring product quality. These procedures enable researchers to comprehensively and accurately identify and assess the quality of Chinese herbal medicines.

#### Authors' contributions

HW and YQL conceived and designed the experiments; YQL and DXX performed the experiments; and HW and YQL analyzed the data and wrote the paper.

#### Conflicts of interest

The authors declare no conflicts of interest.

#### Acknowledgements

This study was supported by the Nature Science Foundation of China (31500261), the Guangdong Province Science and Technology Plan Projects (2014B090904074), and the Youth Foundation of College of Forestry and Landscape Architecture of South China Agricultural University (201603).

#### References

- Abdi, H., Williams, L.J., 2010. Principal component analysis. Wiley Interdiscip. Rev. Comput. Statist. 2, 433–445.
- Aouidi, F., Dupuy, N., Artaud, J., Roussos, S., Msalle, M., Gaime, I.P., Hamdi, M., 2012. Rapid quantitative determination of oleuropein in olive leaves (*Olea europaea*) using mid-infrared spectroscopy combined with chemometric analyses. Ind. Crop. Prod. 37, 292–297.

- Bajpai, V., Kumar, S., Singh, A., Singh, J., Negi, M.P.S., Bag, S.K., Kumar, N., Konwar, R., Kumar, B., 2017. Chemometric based identification and validation of specific chemical markers for geographical, seasonal and gender variations in *Tinospora cordifolia* stem using HPLC-ESI-QTOF-MS analysis. *Phytochem. Anal.* 28, 277–288.
- Beebe, K.R., Pell, R.J., Deascholtz, M.B., 1998. *Chemometrics: A Practical Guide*. Wiley, New York.
- Buchgraber, M., Ulberth, F., Anklam, E., 2004. Cluster analysis for the systematic grouping of genuine cocoa butter and cocoa butter equivalent samples based on triglyceride patterns. *J. Agric. Food Chem.* 52, 3855–3860.
- Bureau, S., Ruiz, D., Reich, M., Gouble, B., Bertrand, D., Audergon, J.M., Renard, C.M.G.C., 2009. Application of ATR-FTIR for a rapid and simultaneous determination of sugars and organic acids in apricot fruit. *Food Chem.* 115, 1133–1140.
- Chen, C.Y., Qi, L.W., Li, H.J., Li, P., Yi, L., Ma, H.L., Tan, D., 2007. Simultaneous determination of iridoids, phenolic acids, flavonoids, and saponins in *Flos Lonicerae* and *Flos Lonicerae Japonicae* by HPLC-DAD-ELSD coupled with principal component analysis. *J. Sep. Sci.* 30, 3181–3192.
- China Pharmacopoeia Commission, 2015a. *Pharmacopoeia of the People's Republic of China 2015*, 1. Chinese Medical Science and Technology Press, Beijing, pp. 30.
- China Pharmacopoeia Commission, 2015b. *Pharmacopoeia of the People's Republic of China 2015*, 1. Chinese Medical Science and Technology Press, Beijing, pp. 221.
- Custers, D., Cauwenbergh, T., Bothy, J.L., Courseille, P., De Beer, J.O., Apers, S., Econink, E.D., 2014. ATR-FTIR spectroscopy and chemometrics: an interesting tool to discriminate and characterize counterfeit medicines. *J. Pharmaceut. Biomed.* 112, 181–189.
- Deconinck, E., Canfyn, M., SacréP, Y., Baudewyns, S., Courseille, P., De Beer, J.O., 2012. A validated GC-MS method for the determination and quantification of residual solvents in counterfeit tablets and capsules. *J. Pharm. Biomed. Anal.* 70, 64–70.
- Demir, P., Onde, S., Severcan, F., 2015. Phylogeny of cultivated and wild wheat species using ATR-FTIR spectroscopy. *Spectrochim. Acta A* 135, 757–763.
- Edelmann, A., Diewock, J., Schuster, K.C., Lendl, B., 2001. Rapid method for the discrimination of red wine cultivars based on mid-infrared spectroscopy of phenolic wine extracts. *J. Agric. Food Chem.* 49, 1139–1145.
- Gao, W., Wang, R., Li, D., Li, K., Chen, J., Li, H.J., Xu, X.J., Li, P., Yang, H., 2016. Comparison of five *Lonicera* flowers by simultaneous determination of multi-components with single reference standard method and principal component analysis. *J. Pharmaceut. Biomed.* 117, 345–351.
- Gao, W., Yang, H., Qi, L.W., Liu, E.H., Ren, M.T., Yan, Y.T., Chen, J., Li, P., 2012. Unbiased metabolite profiling by liquid chromatography-quadrupole time-of-flight mass spectrometry and multivariate data analysis for herbal authentication: classification of seven *Lonicera* species flower buds. *J. Chromatogr. A* 1245, 109–116.
- Gemperline, P., 2006. *Practical Guide to Chemometrics*. Talor & Francis, New York.
- Gok, S., Severcan, M., Goormaghtigh Erik, C., Kandemir, I., Severcan, F., 2015. Differentiation of Anatolian honey samples from different botanical origins by ATR-FTIR spectroscopy using multivariate analysis. *Food Chem.* 170, 234–240.
- Hu, S.Q., Dong, G.L., Chen, X.M., Huang, L.L., Yang, X., Tong, W., 2011. ITS sequence-based identification and utilization evaluation of "Nanjiang" (*Lonicera similis* Hemsl.), a local cultivar in Sichuan, China. *Genet. Resour. Crop. Evol.* 59, 547–555.
- Kim, S., Kim, K.Y., Han, C.S., Ki, K.S., Min, K.J., Zhang, X., Wang, W.K., 2012. Simultaneous analysis of six major compounds in *Osterici radix* and *Notopterygii Rhizoma et Radix* by HPLC and discrimination of their origins from chemical fingerprint analysis. *J. Sep. Sci.* 35, 691–699.
- Kong, D.X., Li, Y.Q., Ba, M., He, H.J., Liang, G.X., Wu, H., 2017. Correlation between the dynamic accumulation of the main effective components and their associated regulatory enzyme activities at different growth stages in *Lonicera japonica* Thunb. *Ind. Crop. Prod.* 96, 16–22.
- Li, D.N., Meng, X.J., Li, B., 2016. Profiling of anthocyanins from blueberries produced in China using HPLC-DAD-MS and exploratory analysis by principal component analysis. *J. Food Compos. Anal.* 47, 1–7.
- Li, Q., Yu, L.J., Deng, Y., 2007. Leaf epidermal characters of *Lonicera japonica* and *Lonicera confusa* and their ecology adaptation. *J. Forest. Res.* 18, 103–108.
- Li, Y.Q., Kong, D.X., Wu, H., 2013. Analysis and evaluation of essential oil components of *cinnamon* barks using GC-MS and FT-IR spectroscopy. *Ind. Crop. Prod.* 41, 269–278.
- Liu, J., Chen, X., Yang, W., Liu, W., Jiang, T., 2010. Study on establishment of RP-HPLC and GC-MS fingerprints for wild germplasm resource of *Ophiopogon japonicus* in Sichuan and hierarchical clustering analysis. *J. Chin. Med. Mater.* 35, 2726–2730.
- Massart, D.L., Vanegiste, B.G.M., Buydens, L.M.C., De Jong, S., Lewi, P.J., Smeyers-Verbeke, J.J., 2007. *Handbook of Chemometrics and Qualimetrics: Part A*. Elsevier, Amsterdam.
- Park, S.C., Lee, S.J., NamKung, H., Chung, H., Han, S.H., Yoon, M.Y., Park, J.J., Lee, J.H., Oh, C.H., Woo, Y.A., 2007. Feasibility study for diagnosis of stomach adenoma and cancer using IR spectroscopy. *Vib. Spectrosc.* 44, 279–285.
- Peng, X.X., Li, W.D., Wang, W.Q., Bai, G.B., 2009. Identification of *Lonicera japonica* by PCR-RFLP and allele-specific diagnostic PCR based on sequences of internal transcribed spacer regions. *Planta Med.* 75, 1–3.
- Pu, Z.M., Xing, J.B., Li, P., Liu, T., Wang, Z.H., 2002. Study on floral morphology of *Flos Lonicerae*. *Chin. Tradit. Herb. Drugs* 25, 854–859.
- Seo, O.N., Kim, G.S., Park, S., Lee, J.H., Kim, Y.H., Lee, W.S., Lee, S.J., Kim, C.Y., Jin, J.S., Choi, S.K., Shin, S.C., 2012. Determination of polyphenol components of *Lonicera japonica* Thunb. using liquid chromatography-tandem mass spectrometry: contribution to the overall antioxidant activity. *Food Chem.* 134, 572–577.
- Shang, X.F., Pan, H., Li, M.X., Miao, X.L., Ding, H., 2011. *Lonicera japonica* Thunb.: ethnopharmacology, phytochemistry and pharmacology of an important traditional Chinese medicine. *J. Ethnopharmacol.* 138, 1–21.
- Su, S., Hua, Y., Duan, J.A., Shang, E., Tang, Y., Bao, X., Lu, Y., Ding, A., 2008. Hypothesis of active components in volatile oil from a Chinese herb formulation 'Shao-Fu-Zhu-Yu decoction', using GC-MS and chemometrics. *J. Sep. Sci.* 31, 1085–1091.
- Sun, S.Q., Zhou, Q., Chen, J.B., 2010. *Analysis of Traditional Chinese Medicine by Infrared Spectroscopy*. Chemical Industry Press, Beijing, pp. 23–25.
- Sun, Z.Y., Gao, T., Yao, H., Shi, L.C., Zhu, Y.Z., Chen, S.L., 2011. Identification of *Lonicera japonica* and its related species using the DNA barcoding method. *Planta Med.* 77, 301–306.
- Tistaert, C., Dejaeger, B., Nguyen Hoai, N., Chataigné, G., Rivière, C., Nguyen, T.H., Chau, V.M., Quettin-Leclercq, J., Vander Heyden, Y., 2009. Potential antioxidant compounds in *Mallotus* species fingerprints Part I: indication, using linear multivariate calibration techniques. *Anal. Chim. Acta* 652, 189–197.
- Wang, C.Z., Li, P., Ding, J.Y., Fishbein, A., Yunb, C.S., 2007. Discrimination of *Lonicera japonica* Thunb. from different geographical origins using restriction fragment length polymorphism analysis. *Biol. Pharm. Bull.* 30, 779–782.
- Wang, Q.X., Quan, Q.M., Zhou, X.L., Zhu, Y.G., Lan, Y.L., Li, S., Yu, Y., Cheng, Z.A., 2014. Comparative study of *Lonicera japonica* with related species: morphological characteristics ITS sequences and active compounds. *Biochem. Syst. Ecol.* 54, 198–207.
- Wang, X., Sheng, D.P., Zhu, Z.J., Xu, F.C., Huang, D., Yu, C.J., 2015. Identification of *Cortex Eucommiae* from different producing areas by FTIR microspectroscopy. *Spectrochim. Acta A* 141, 94–98.
- Wold, S., 1976. Pattern recognition by means of disjoint principal components models. *Pattern Recogn.* 8, 127–139.
- Wu, Y.W., Sun, S.Q., Zhou, Q., Leung, H.W., 2008. Fourier transform mid-infrared (MIR) and near-infrared (NIR) spectroscopy for rapid quality assessment of Chinese medicine preparation Honghua Oil. *J. Pharmaceut. Biomed.* 46, 498–504.
- Xu, B.S., Hu, J.Q., Wang, H.J., 1988. *Flora of China*, 72. Science Press, Beijing, pp. 143–259.
- Yuan, Y., Song, L.P., Li, M.H., Liu, G.M., Chu, Y.N., Ma, L.Y., 2012. Genetic variation and metabolic pathway intricacy govern the active compound content and quality of the Chinese medicinal plant *Lonicera japonica* Thunb. *BMC Genomics* 13, 1–17.
- Zhu, Y., Xu, C.H., Huang, J., Li, G.Y., Liu, X.H., Sun, S.Q., Wang, J.H., 2014. Rapid discrimination of cultivated *Codonopsis lanceolata* in different ages by FT-IR and 2DCOS-IR. *J. Mol. Struct.* 1069, 272–279.